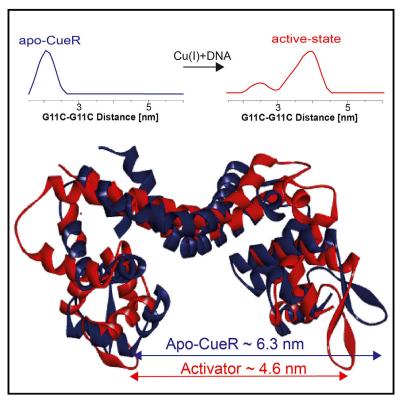# Structural and Dynamics Characterization of the MerR Family Metalloregulator CueR in its Repression and Activation States

Graphical Abstract

Authors

Hila Sameach, Aya Narunsky, Salome Azoulay-Ginsburg, ..., Tamar Juven-Gershon, Nir Ben-Tal, Sharon Ruthstein

Correspondence

sharon.ruthstein@biu.ac.il

In Brief

Sameach et al. utilize spectroscopy measurements and structure modeling to resolve the structural and dynamic changes that the CueR metalloregulator undergoes when binding copper and DNA. They show that CueR's N-terminal domain is highly dynamic and assumes substantial conformational changes upon copper and DNA coordination.

Highlights

- A mechanistic picture for the CueR metalloregulator is provided

- The mechanism shows the dependence of CueR activity on Cu(I) concentration

- A combination of DEER spectroscopy and structure modeling predicts CueR's dynamics

CellPress

Structural and Dynamics Characterization of the MerR Family Metalloregulator CueR in its Repression and Activation States

Hila Sameach,[1,4] Aya Narunsky,[2,4] Salome Azoulay-Ginsburg,[1] Lada Gevorkyan-Aiapetov,[1] Yonathan Zehavi,[3] Yoni Moskovitz,[1] Tamar Juven-Gershon,[3] Nir Ben-Tal,[2] and Sharon Ruthstein[1,5,*]

[1]The Chemistry Department, Faculty of Exact Sciences, Bar Ilan University, Ramat-Gan 5290002, Israel
[2]Department of Biochemistry and Molecular Biochemistry, George S. Wise Faculty of Life sciences, Tel Aviv University, Ramat Aviv 69978, Israel
[3]The Mina and Everard Goodman Faculty of Life Sciences, Bar Ilan University, Ramat-Gan 5290002, Israel
[4]These authors contributed equally
[5]Lead Contact
*Correspondence: sharon.ruthstein@biu.ac.il
http://dx.doi.org/10.1016/j.str.2017.05.004

SUMMARY

CueR (Cu export regulator) is a metalloregulator protein that "senses" Cu(I) ions with very high affinity, thereby stimulating DNA binding and the transcription activation of two other metalloregulator proteins. The crystal structures of CueR when unbound or bound to DNA and a metal ion are very similar to each other, and the role of CueR and Cu(I) in initiating the transcription has not been fully understood yet. Using double electron-electron resonance (DEER) measurements and structure modeling, we investigate the conformational changes that CueR undergoes upon binding Cu(I) and DNA in solution. We observe three distinct conformations, corresponding to apo-CueR, DNA-bound CueR in the absence of Cu(I) (the "repression" state), and CueR-Cu(I)-DNA (the "activation" state). We propose a detailed structural mechanism underlying CueR's regulation of the transcription process. The mechanism explicitly shows the dependence of CueR activity on copper, thereby revealing the important negative feedback mechanism essential for regulating the intracellular copper concentration.

INTRODUCTION

Metals are essential for the survival of all cells, whether prokaryotic or eukaryotic; however, metal ions can be highly toxic as well. Bacterial cells have developed a sophisticated mechanism to regulate the concentration of metal ions within their cytoplasm (Changela et al., 2003; Finney and O'Halloran, 2003; Robinson and Winge, 2010; Wladron et al., 2009). One key factor in this mechanism is a family of metal sensors, called metalloregulators, which sense specific metal ions with high affinity and specificity, and consequently control the concentration of these metal ions within the cell (Brown et al., 2003; Ma et al., 2009). CueR (Cu export regulator) is an *Escherichia coli* protein that belongs to the MerR family of

metalloregulators, and senses the Cu(I) ion with 10^{-21} M affinity. When CueR that is bound to DNA recognizes (and binds) Cu(I), it induces the transcription of two proteins (Changela et al., 2003; Outten et al., 2000): The first is CopA (Stoyanov et al., 2001), which removes Cu(I) from the cytosol into the periplasm, and the second is CueO, a cytoplasmic protein that oxidizes Cu(I) to the less toxic Cu(II) form (Grass and Rensing, 2001).

CueR's mechanism of inducing transcription is generally understood to operate as follows. Both the apo and holo states of CueR can bind to a specific DNA sequence within a promoter (Andoy et al., 2009). However, in the absence of metal, the metalloregulator bends the DNA such that the RNA polymerase cannot interact with the CopA promoter properly, thereby repressing transcription (Outten et al., 1999). Upon metal coordination, CueR enables the DNA to assume a conformation that can activate the transcription process. Using single-molecule fluorescence resonance energy transfer (FRET) measurements, Chen's group has shown that it is possible to turn off the transcription process by substituting holo-CueR (bound to Cu(I)) with apo-CueR protein (Joshi et al., 2012). Chen's study also suggests that CueR has a dynamic nature and it can assume various conformational states that assist in the transcription process. Recently, Philips et al. (2015) reported a crystal structure of CueR-Ag(I)-DNA and also characterized a structure in which the metal-binding site C112-Ag(I)-C120 had been mutated to S112-S120, which repressed transcription activity. The crystal structures of Cu(I)-CueR (Changela et al., 2003) and Ag(I)-CueR were found to be similar. The authors showed that the largest difference between these two complexes lies in the DNA conformation, which is stabilized by two slightly different conformational states of CueR. However, for other metalloregulators from the MerR family, such as the *Bacillus subtilis* MtaN (Newberry and Brennan, 2004) and the BmrR protein (Kumaraswami et al., 2010), different conformations were adopted by the protein in the presence and absence of DNA. To resolve the CueR transcription mechanism, and the role of Cu(I) in initiating the transcription, it is essential to monitor the protein's flexibility in solution upon coordinating Cu(I) and binding to DNA. Herein, we sought to provide a more fine-grained understanding of the mechanism by which CueR activates and represses the transcription process.
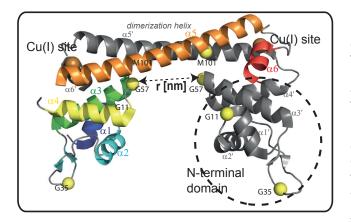
Figure 1. The Cu(I)-CueR Homodimeric Structure, PDB: 1Q05
The residues of the spin-labeled sites are marked using yellow α carbon atoms-spheres representation, and the Cu(I) ions are represented as orange spheres. The dashed circle denotes the N-terminal domain of the rightmost subunit.

Over the last decade, double electron-electron resonance (DEER) spectroscopy coupled with site-directed spin labeling (SDSL) has been found to be an excellent means of obtaining structural and dynamic information on complex systems (Aitha et al., 2015; Bhatnagar et al., 2012; Freed et al., 2013; Jeschke, 2012; Joseph et al., 2014; Klare, 2013; Sahu et al., 2013). Hubbell's group was the first to introduce the SDSL methodology, in which nitroxide spin labels are attached to cysteine residues at selected positions within the protein (Hubbell et al., 1998, 2013). The most common nitroxide spin label used is the 1-oxyl-2,2,5,5-tetramethylpyrroline-3-methyl methanethiosulfonate spin label (MTSSL). DEER, also called pulsed electron double resonance, is a pulsed electron paramagnetic resonance (EPR) technique used to measure the dipolar interactions between two or more electron spins; thus, it can provide nanometer interspin distance information in the range of 1.5–8.0 nm. Such information can reveal conformational changes such as those we seek to identify. For example, using DEER and SDSL, Puljung et al. (2014) discovered major conformational changes in the HCN channel upon ligand binding, which could not have been observed by X-ray crystallography or FRET. DEER spectroscopy has also been used to reveal structural differences between EcoR1 that is bound to a non-specific DNA sequence versus EcoR1 bound to a specific DNA sequence (Stone et al., 2008). In addition, Butala et al. (2011) used DEER spectroscopy to show that the *E. coli* dimeric LexA transcriptional repressor is more flexible in the unbound state than in the DNA-bound state.

We utilized the benefits of DEER spectroscopy to target the conformational changes that CueR assumes upon DNA coordination. We combined DEER spectroscopy with elastic-network calculations and ConTemplate structural modeling (Polyhach et al., 2011; Narunsky et al., 2015) to gain knowledge about CueR's conformational state when it is in complex with Cu(I) and DNA, compared with apo-CueR. We show that the interaction with DNA and Cu(I) induces conformational changes in the DNA-binding N-terminal domain of CueR. These observations advance our understanding of the transcription mechanism underlying the cellular regulation of Cu(I) concentration.
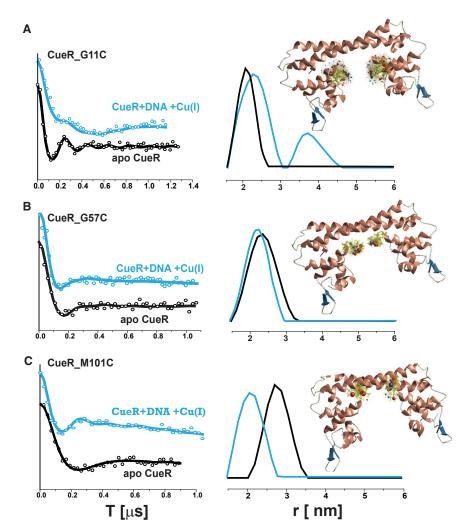
RESULTS

Generation of Mutants for Spin Labeling
The CueR protein is a dimer in which each monomer contains six helices: α1 to α4 make up the N-terminal, DNA-binding domain, and α5 and α6 compose the C-terminal domain; the turn between the latter two helices forms the metal-binding site (Figure 1) (Changela et al., 2003; Giedroc and Arunkumar, 2007). Each CueR monomer contains four cysteine residues: C112, C120, C129, and C130. Of these, C112 and C120 form the Cu(I) metal-binding site through linear Cu(I) dithiolate coordination. Mutations of C112 or C120 have been shown to abrogate all responses of CueR in vivo (Stoyanov and Brown, 2003) and in vitro (Chen et al., 2003). On the other hand, C129 and C130 were shown to be non-essential for the transcription process, indicating that they are not critical for metal ion coordination (Stoyanov and Brown, 2003). Notably, the latter two residues are also missing from the CueR crystal structure (Changela et al., 2003). We found that the C129 and C130 residues are accessible to spin labels; thus, in our experiments we mutated both to alanine (C129A, C130A) to prevent spin labeling at these sites. Run-off transcription assays (see Figure S1C) confirmed that these mutations do not interfere with transcription. To target conformational changes that the protein assumes in the presence of a specific DNA sequence, we generated several mutations (see Figure S1A in the Supplemental Information): G11C is between α1 and α2; G57C is between α3 and α4; M101C is on α5; and G11C + G35C are in the N-terminal domain, where G35C is situated in the turn between α2 and α3 (the corresponding mutant proteins are referred to as CueR_G11C, etc.). Circular dichroism spectra confirm that these point mutations do not alter the secondary structure of the protein (Figure S1D). Several experiments (electrophoresis mobility shift assay) by fluorescence and pull-down experiments (Figure S2) confirm that the spin-labeled mutant proteins bind the promoter, similarly to the wild-type CueR protein (WT-CueR).

Comparison between CueR-Cu(I)-DNA and Apo-CueR
We performed DEER experiments on spin-labeled CueR in the presence and absence of Cu(I) and DNA. The DEER signals and the corresponding distance distribution functions are presented in Figure 2 (blue curves correspond to CueR-Cu(I)-DNA, and black curves correspond to apo-CueR). Figure 2 shows that the DEER signals were greatly affected by the presence of DNA and Cu(I).

The DEER experiments on CueR_G11C (Figure 2A) revealed a distance distribution of 2.1 ± 0.3 nm. In the presence of DNA and Cu(I), CueR_G11C assumed two conformational states: one was somewhat similar to the conformation obtained in the absence of DNA and Cu(I), corresponding to a distance distribution of 2.4 ± 0.5 nm, and the other corresponded to a distribution of around 3.8 ± 0.5 nm. Since the DEER assay is performed in solution, the distance distribution function derived from the DEER signal takes into account all orientations of the spin label. Therefore, the second distribution around 3.8 nm indeed reflects a different conformation of the protein and is not merely a result of the spin-label orientation.

Figure 2B shows the DEER signals and the corresponding distance distribution functions for CueR with a spin label at the

A

Figure 2. Monitoring the Inter-monomer Conformational Changes Induced by Cu(I) and DNA Binding

DEER signals and the corresponding distance distribution functions in apo-CueR (solid black curve) and in the presence of DNA and Cu(I) (solid blue curve, in a ratio of 1:1:3 CueR:DNA:Cu(I)) for: (A) CueR_G11C, (B) CueR_G57C, and (C) CueR_M101C. The insets in all panels show the structure of the PDB: 1Q05 CueR dimer with the distribution of the spin label conformers attached to the selected cysteine residues, obtained from MMM2015 simulations. Upon DNA and Cu(I) co-ordination, the two G11C residues spread apart, whereas the M101C residues get closer to each other.

CueR monomer) of Cu(I) was included in the solution, the distance distribution shifted slightly to 2.2 ± 0.3 nm. In the presence of three equivalents of Cu(I), CueR showed a similar conformational state, with a slightly narrower distance distribution of 2.2 ± 0.2 nm. These observations indicate that Cu(I) slightly rigidifies the structure of CueR.

The addition of DNA alone to the CueR solution resulted in a broad distance distribution of 2.0–3.5 nm. Theoretically, the broader distribution could result from increased flexibility of CueR upon DNA binding, but such an increase would be highly unlikely. Rather, we suggest that the broadening is indicative of the presence of two populations: some of the CueR molecules are bound to the DNA in solution, whereas others remain unbound. Indeed, using single-molecule FRET, Chen and colleagues recently showed in vitro, and in cell, that in the presence of DNA there is equilibrium between bound CueR and unbound CueR, and that, in solution, a continuous shift between the two groups of molecules is observed (Chen et al., 2015; Martell et al., 2015). Given that CueR regulates Cu(I) concentration by influencing transcription, we explored the possibility that changes in Cu(I) concentration might influence this equilibrium. The presence of one equivalent of Cu(I) in the CueR and DNA solution preserved the conformational states observed in the presence of DNA alone. However, in the presence of three equivalents of Cu(I), an additional conformational state emerged, with a distance distribution of around 3.8 ± 0.5 nm. In the presence of four equivalents of Cu(I), the contribution of the latter conformation to the distance distribution function increased. It is worth mentioning that our results reflect CueR's behavior in vitro; by using an excess of Cu(I) concentrations, we were able to monitor this behavior and observe trends in the metalloregulator's structural changes. The conformational differences observed under different concentrations of Cu(I) indicate that copper can dissociate from CueR in vitro.

These results suggest that there are distinct differences among the conformations of apo-CueR, DNA-bound CueR (the

G57C site. In this case we observed a similar distance distribution in the presence and absence of DNA and Cu(I), with values around 2.3 ± 0.4 nm, suggesting that this region of the protein is less affected by the presence of DNA and Cu(I). When a spin label was introduced at M101C (Figure 2C), the DEER showed a distance distribution of 2.8 ± 0.5 nm in the absence of DNA and Cu(I), and a distance distribution of 2.1 ± 0.4 nm in the presence of DNA and Cu(I). These observations suggest that the spin labels attached to M101C draw closer together upon binding of DNA and Cu(I).

In sum, the DEER data suggest that the region corresponding to the spin-labeled site G11C undergoes large conformational changes upon DNA and Cu(I) binding. In contrast, G57C is insensitive to the presence of DNA and Cu(I), and the region corresponding to M101C undergoes minor structural changes in the presence of DNA and Cu(I).

The Effects of Cu(I) or DNA Alone on the CueR Structure

To explore the effects of Cu(I) alone and of DNA alone on CueR structure, we acquired the DEER signals for the CueR_G11C mutant in the presence of DNA and different concentrations of Cu(I) (Figure 3). For apo-CueR the average distance distribution was 2.1 ± 0.3 nm; when one equivalent (i.e., one equivalent per
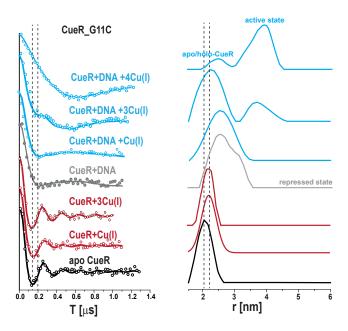
Figure 3. The Effects of DNA and Cu(I) Concentration
DEER signals and the corresponding distance distributions for the CueR_G11C mutant in the presence and absence of DNA and various concentrations of Cu(I). Clear differences are observed among the conformational states of apo-CueR (black line), Cu(I)-CueR (red line), CueR-DNA (gray line), and CueR-Cu(I)-DNA (blue line).

"repression" state of the protein), and CueR bound to Cu(I) and DNA (the "activation" state). Whereas in apo-CueR the distance distribution between the two G11C spin labels was 2.1 ± 0.3 nm, the repression state conformation (CueR-DNA) corresponds to an inter-monomer distance between 2.0 and 3.5 nm, and the activation state conformation (CueR-Cu(I)-DNA) corresponds to a distance distribution of 3.8 ± 0.5 nm. The distance distribution corresponding to the active state is broader than that corresponding to the apo state. This suggests that, in line with the single-molecule results of Chen and colleagues (Martell et al., 2015), multiple conformational states of Cu(I)-DNA-CueR can exist in solution, while only one conformation can eventually lead to a transcription process. In particular, our experiments suggest that, in the presence of DNA, there is an equilibrium between molecules of apo-CueR, CueR-DNA complexes and Cu(I)-CueR-DNA complexes; the concentration of Cu(I) influences this equilibrium, such that, as the concentration increases, a greater proportion of CueR-bound DNA is in the activation state (Cu(I)-CueR-DNA complex). Thus, the probability to initiate transcription depends on the Cu(I) concentration, an essential characteristic of CueR as a metal sensor regulating this ion's concentration. Chen's group (Martell et al., 2015) reported that CueR represses and activates transcription via modulation of RNA polymerase interaction with DNA; it seems likely that the conformational differences we observed between CueR's repression and activation states relate to this modulation.
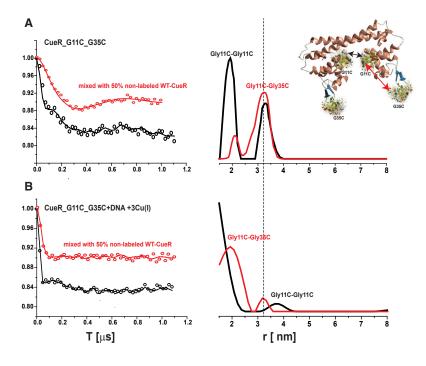
X-ray crystal structures of CueR support our observations that the inter-monomer distances of the G11 residues vary across the protein's various states. The crystal structure of Cu(I)-CueR (PDB: 1Q05) shows an inter-monomer distance of 4.03 nm be-

tween the α carbons of the dimer's two G11 residues. The crystal structure of Ag(I)-CueR (PDB: 1Q06) indicates a similar distance. In the crystal structure of CueR-DNA (PDB: 4WLS) the G11-G11 inter-monomer distance is about 1.0 nm shorter, at 3.02 nm. When Ag(I) is included in the complex (crystal structure of Ag(I)-CueR-DNA, PDB: 4WLW), the distance increases to 4.06 nm. These differences suggest that the corresponding region of CueR is sensitive to DNA binding.

Our DEER measurements indicate even larger conformational changes in CueR upon binding to DNA and Cu(I). Specifically, the average inter-monomer distance between two spin labels attached to G11C is about 1.0–1.5 nm longer in the activation state than in the apo state, suggesting that the two α1 helices spread apart. The difference between the DEER measurements and the distances observed in the crystal structure may be attributable to the fact that DEER, which is carried out on the entire protein in solution, can target conformational states that are unobservable in crystal structures.

Exploring the Intra-monomer Conformational Changes in the DNA N-Terminal Domain

To examine the intra-monomer conformational changes that are induced by DNA and Cu(I) binding, we introduced two spin labels at positions G11C and G35C. Figure 4 shows the DEER signals and corresponding distance distribution functions in the absence and presence of DNA and Cu(I) (black solid lines). Performing DEER measurements on a multispin system (n > 2) is not trivial and requires careful analysis. We expected to be able to detect only the G11C-G11C inter-monomer distance distribution and the G35C-G11C intra-monomer distance distribution. Longer distances, corresponding to the inter-monomer G11C-G35C and G35-G35C distances, could not be measured in these experiments because of the short timescale of the DEER signal.

Indeed, a bimodal distance distribution function was obtained. One peak of around 2.0 ± 0.3 nm was detected, similar to that observed in the CueR_G11C mutant; this peak corresponded to the G11C-G11C inter-monomer distance distribution function. A second peak was obtained at 3.4 ± 0.3 nm; we suspected that this peak corresponded to the intra-monomer distance between G11C and G35C. To confirm this hypothesis, we randomly mixed the spin-labeled CueR_G11C_G35C solution with 50% unlabeled WT-CueR (i.e., CueR monomers could spontaneously mix in the solution to form new dimers; the spin-labeled CueR concentration was about 5 μM). In the diluted solution (WT-CueR/CueR_G11C_G35C), the contribution of the inter-monomer G11C-G11C distance distribution was expected to decrease, while the contribution of the intra-monomer G11C-G35C distance distribution was expected to remain the same, such that the dominant peak would correspond to the G11C-G35C intra-monomer distance distribution. The DEER signal and corresponding distance distribution function are plotted in red in Figure 4A. The mixed solution provided a pronounced distance distribution function of 3.3 ± 0.3 nm, which could thus be associated with the intra-monomer G11C-G35C distance distribution. Moreover, a decrease in the two-pulse (2p) field-sweep echo spectral width was observed upon dilution with unlabeled protein, from 172 ± 2.0 to 147 ± 2.0 G, consistent with the decrease in distances smaller than 2.0 nm.

A

CueR_G11C_G35C

mixed with 50% non-labeled WT-CueR

Gly11C-Gly11C

Gly11C-Gly35C

B

CueR_G11C_G35C+DNA +3Cu(I)

mixed with 50% non-labeled WT-CueR

Gly11C-Gly35C

Gly11C-Gly11C

T [μs]

r [nm]

Figure 4. Monitoring the Intra-Monomer Conformational Changes Induced by Cu(I) and DNA Binding

DEER signals and corresponding distance distribution functions (black solid lines) for the CueR_G11C_G35C mutant. (A) In the apo form. (B) In the presence of DNA and Cu(I). Red solid lines represent spin-labeled CueR_G11C_G35C mixed with 50% non-labeled WT-CueR. The inset shows the structure of the PDB: 1Q05 CueR dimer with the distribution of spin label conformers attached to selected cysteine residues, obtained from MMM2015 simulations. Upon DNA and Cu(I) binding the intra-monomer distance between G11C and G35C shortens.

In the presence of DNA and Cu(I), a larger contribution of distances smaller than 2.0 nm was observed (the 2p field-sweep echo spectral width increased to 190 ± 2.0 G). In addition, we detected a peak of 3.8 ± 0.6 nm, similar to the distribution obtained for the CueR_G11C mutant in the presence of DNA and Cu(I) (the blue curve in Figure 2A). We also acquired the DEER signal of the mixed solution of spin-labeled and unlabeled CueR, and a clear distribution around 2.1 ± 0.4 nm was obtained, which we associated with the intra-monomer G11C-G35C distance distribution in CueR's activation state (the 2p field-sweep echo-detected spectral width of 166 ± 2.0 G). A small population of CueR molecules with a distance of 3.3 ± 0.3 nm was also apparent; as noted above, we suggest that these molecules are not bound to DNA, confirming the presence of both DNA-bound and unbound populations. The DEER data imply that upon DNA and Cu(I) binding, the intra-monomer distance between G11C and G35C decreases tremendously, resulting in a shift of the average G11C-G35C intra-monomer distance from 3.3 to 2.1 nm.

Comparison of CueR Crystal Structures with Models Based on DEER Measurements

Taken together, our DEER data suggest that DNA binding and Cu(I) binding induce conformational changes in the two N-terminal DNA-binding domains of the dimer. These changes induce an increase in the inter-monomer distance between the two spin labels attached to the G11C residues, and a decrease in the intra-monomer distance between the two spin labels attached to G11C and G35C. In addition, we observed a slight conformational change in the α5 helix of the protein (the M101 site).

We used the five DEER constraints, namely, the three inter-monomer distance distributions and two intra-monomer distance distributions, to create a structure for apo-CueR and for the CueR-Cu(I)-DNA complex by utilizing the elastic-network model implemented in the multiscale modeling of macromolecular systems (MMM2015 computations) software. CueR is a relatively small protein, and thus five distance distribution constraints are sufficient in order to create a structure model. The structure of Cu(I)-CueR (PDB: 1Q05) was used as input for the modeling. Figure 5A presents the apo-CueR structure created based on the DEER constraints (dark blue) overlaid on the PDB: 1Q05 structure (light blue). The DEER structure for the apo-CueR suggests some bending in the α5 dimerization helix, which results in a less symmetric structure compared with the crystal structure. In addition, the two structures differ in the DNA-binding domain and, specifically, in the orientation of the α1-α2 helices with respect to the α3 helix. Figure 5B presents the DEER structure for the CueR-Cu(I)-DNA complex (red) overlaid on the PDB: 1Q05 structure (light blue), and Figure 5C presents the DEER model structure for the CueR-Cu(I)-DNA complex (red) overlaid on the crystal structure of CueR-Ag(I)-DNA (green; PDB: 4WLW). The DNA-binding domain in the DEER-based model structure is more consistent with the 4wlw crystal structure (CueR-Ag(I)-DNA) than with the PDB: 1Q05 crystal structure, as reflected in the orientation of the α1-α3 helices with respect to each other. Figure 5D shows the two DEER model structures (apo-CueR, blue; and CueR-Cu(I)-DNA, red) overlaid on each other. It indicates that, in the active state, the two DNA-binding domains are about 1.7 nm closer to each other than in the apo state. This measurement reflects the inter-monomer distance between the α carbons of the two G35 residues; see Table S1 in Supplemental Information. In addition, the two α1 helices spread apart upon DNA and Cu(I) binding, pushing the α2 helix toward the α3 helix.

Predicted Conformational Changes

The DEER data indicate that CueR can assume various conformations that are associated with the activation and repression of the transcription process. As discussed above, the structures suggested by the DEER experiments (for the apo and activation states) are different from the crystal structures for the CueR protein. Yet, as experimental methods are limited in terms of their resolution and sensitivity, it is possible that even these structures do not provide a comprehensive picture of the conformations of CueR. Hence, to further explore CueR's conformational space, we queried the ConTemplate web-server (http://bental.tau.ac.il/contemplate) with the crystal structure of Cu(I)-CueR, PDB: 1Q05. ConTemplate exploits the wealth of structural data in the PDB and suggests alternative conformations for a given
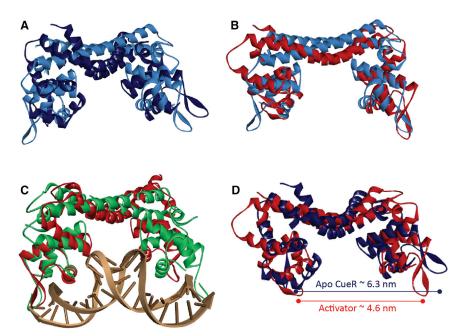
query. It suggested the following structural templates as alternative conformations for CueR: PDB: 1Q06 (Ag(I)-CueR); three structures of Zn(II)-ZntR: PDB: 1Q08, 1Q09, and 1Q0A; 1JBG (MtaN), 1R8D (MtaN bound to DNA), 2ZHH ([2Fe-2S]-SoxR), 2ZHG ([2Fe-2S]-SoxR bound to DNA), 4UA1 (MerR from *Bacillus megaterium* MB1), and 4WLW (CueR-Ag(I)-DNA). Reassuringly, these crystal structures are all related to the metalloregulator MerR family. Homology models of CueR were obtained using these structures as templates, and we used the MMM program to simulate the attachment of MTSSL to specific residues within these model structures, and to compute the corresponding distance distribution functions. Figures 6 and S6, in the Supplemental Information show the possible distribution functions obtained for the suggested structures.

Similar conformational states within ±0.5 nm were obtained for the following structures: PDB: 1Q06, 1Q08, 1Q09, 1R8D, 1JBG, 4UA1, 4WLW, 2ZHH, and 2ZHG (Figure 6). The structure of PDB: 1Q0A is different from the other conformations, since it is an "open" version of PDB: 1Q05, i.e., a structure in which the dimer is in an open state. Hence, the distance distribution function obtained for PDB: 1Q0A is completely different from the one observed for PDB: 1Q05 and our experimental data (see Figure S6). Taking into account all the conformations, these structures can provide an indication for the range of the possible dynamics of the CueR protein.

Summing up the distances obtained both experimentally and through structure modeling, we observe that the inter-monomer distance between two spin labels attached to G11C can be in the range of 4.5 ± 1.5 nm. We note that, while the inter-monomer distance between the G11C residues in the CueR-Cu(I)-DNA complex is consistent with the various crystal structures, the inter-monomer G11C-G11C distance for the apo-CueR obtained from the DEER is not consistent with the crystal structures. Indeed, Figure 5 shows that the crystal structure of Cu(I)-CueR (PDB: 1Q05) is less similar to the DEER-based model for the apo-CueR than to the DEER-based model of the CueR-Cu(I)-

DNA complex. We further observe that the inter-monomer distance between two spin labels attached to the G57C residues (Figure 6B) can be in the range of 1.9 ± 0.9 nm. Similarly, spin labels attached to M101C (Figure 6C) indicate an inter-monomer M101C-M101C distribution (dynamic range) of 2.1 ± 1.1 nm in the presence of DNA and Cu(I). The range indicated by ConTemplate for the intra-monomer distance between spin labels attached to G11C and to G35C (Figure 6D) is 3.5 ± 0.5 nm for most of the crystal structures, with the exception of PDB: 4UA1. DEER produced this intra-monomer distance distribution only for the apo-CueR state (see Figure 4B). For the activation state, DEER indicated a G11C-G35C distance distribution of 2.1 ± 0.4 nm, which is close to that observed in 4ua1 structure. Overall, the dynamics ranges obtained from ConTemplate and from the DEER data suggest that spin labels attached to G11C have slightly broader range of conformations compared with spin labels attached to G57C or M101C.

Figure 6E shows the PDB: 1Q05 conformation (PDB: 1Q05, red) overlaid on four of the conformations suggested by ConTemplate: PDB: 1R8D, 1Q09, 2ZHG, and 4UA1 (gray). As shown in the figure, the regions that undergo the largest changes in structure and conformation are those corresponding to the DNA-binding N-terminal domain of CueR and the hinge that connects the Cu(I) binding site to the DNA-binding N-terminal domain. This observation is consistent with the DEER data, which show that residues in this region (G11 and G35) acquire the largest changes in their conformation upon coordinating to DNA and Cu(I).

DISCUSSION AND CONCLUSIONS

Herein, we utilized DEER, elastic-network analysis, and homology modeling to gain insight into the structural flexibility of the CueR metal sensor from the MerR family upon Cu(I) and DNA binding. An understanding of the function of this class of proteins can shed light on the mechanisms by which microorganisms survive in mammalian hosts, and can assist in the development of suitable antibiotics.
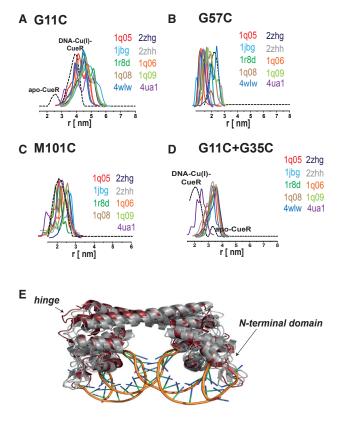
Figure 6. Dynamics Predictions Using ConTemplate

The distance distribution functions derived from the MMM simulations on the suggested conformations obtained using ConTemplate, overlaid on the DEER experimental data for CueR mutants in the presence of DNA and Cu(I) (black dashed line) for: (A) CueR_G11C, (B) CueR_G57C, (C) CueR_M101C, (D) CueR_G11C_G35C spin labeled only on one monomer, and (E) the PDB: 1Q05 structure (red) overlaid on the PDB: 1R8D, 1Q09, 2ZHG, and 4UA1 homology models (gray). The black arrows denote the regions that are most dynamic and flexible (see also Figure S6).

We spin labeled sites in the following regions in the CueR protein and obtained their corresponding distance distribution functions: the α5 dimerization helix (M101C site), the region between the α3 and α4 helices (the G57C site), and the DNA-binding domain (the G11C and G35C sites). In the presence of DNA and Cu(I), the largest structural changes were observed in the DNA-binding domain, where the average inter-monomer distance between two spin labels attached to G11C increased by about 1.5–2.0 nm, and the average intra-monomer distance between spin labels attached to G11C and G35C decreased by about 1.0–1.5 nm. Notably, we also observed structural changes in the long α5 helix, which is close to the Cu(I) binding sites; these included alterations in the conformations of spin labels attached to M101C residues. The CueR_G57C site, which is located closer to the α4 helix, showed little structural change upon Cu(I) and DNA binding.

We also investigated the structure of the CueR_G11C mutant in the presence of either Cu(I) or DNA alone. The data suggest that CueR resides in three different conformational states: the apo-CueR state, the CueR-DNA state (repression state), and the CueR-Cu(I)-DNA state (activation state). When we incremen-

tally increased the concentration of Cu(I) in a solution containing CueR_G11C and DNA, we observed that the protein population included a blend of DNA-Cu(I)-bound and unbound states of CueR. At the highest concentration of copper, the DNA-Cu(I)-bound state dominated. The relatively large distance distribution obtained for the Cu(I)-DNA-CueR state indicates that this state can accommodate various conformations. Our observations confirm that copper is indeed the main trigger that induces the protein to shift from a repression state into an activation state, thereby initiating transcription.

On the basis of the DEER constraints, we produced model structures for apo-CueR and CueR-Cu(I)-DNA in solution. These structures showed trends that corresponded to the crystallographic data obtained for CueR; however, the models also differed from the crystal structures somewhat. Although these are model structures, which should be refined (e.g., based on additional DEER constraints), the large structural changes observed using DEER, which were not observed by crystallography, can only be attributed to the fact that the DEER data were acquired in solution, where the different conformational states of the protein could be targeted.

The observed distances between G35 and G35 can provide indications about the changes that take place in the DNA-binding domains of CueR (Table S1). The DEER data indicated that the distance between the two DNA-binding domains of the dimer decreases by about 1.7 nm upon DNA and Cu(I) binding (Figure 5D). Accordingly, results obtained by crystallography showed a shift of 0.6 nm upon promoter activation (PDB: 4WLW, 4WLS). Other MerR-related crystal structures demonstrate the same trend: MtaN (PDB: 1JBG, 1R8D) shifts by about 1.2 nm upon DNA binding; SoxR (PDB: 2ZHH, 2ZHG) shifts by 0.4 nm; and BmrR shifts by 2.0 nm. DNA-bound and unbound states of BmrR also show clear difference in the orientation of the α1-α4 helices, similar to the difference detected in CueR in our DEER experiments (Kumaraswami et al., 2010). Hence, the observed structural changes accommodated by CueR can twist the DNA and ultimately enable transcription initiation.

To gain a broader perspective on CueR's conformational space, we used ConTemplate to identify structural homologs of the protein, and then compared the DEER data with MMM simulation data corresponding to the various homologs. According to this analysis, the region with the lowest similarity across the various structures corresponded to CueR's DNA-binding domain. This observation is consistent with the idea that this region is highly sensitive to DNA binding and can accommodate multiple conformational states.

Notably, although our DEER data indicated that the apo-CueR and CueR-Cu(I)-DNA states differ substantially from each other in terms of the inter-monomer G11C-G11C distance and the intra-monomer G11C-G35C distance, no such differences were reflected in the various crystal structures we analyzed. Given that various biochemical assays (see Figure S2) have confirmed that spin-labeled mutants bind DNA similarly to WT-CueR, we believe that the discrepancy between the DEER data and the crystallographic data is a result of the fact that the DEER data were acquired in solution, and thus were able to target additional, less symmetric conformations.

On the basis of our data, we suggest the following mechanism for transcription repression/activation: DNA binding to apo-CueR
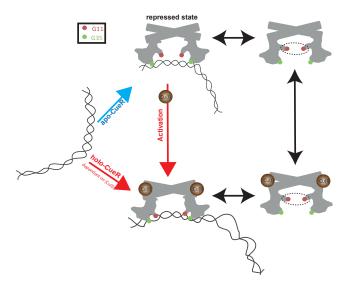
Figure 7. The CueR Activation Mechanism
The brown dots denote the G11 residues, and the green dots denote the G35 residues. In the activation state, the intra-monomer distance between G11 and G35 is shorter, whereas the inter-monomer distance between the two G11 residues is longer.

causes the dimer's two α1 helices to somewhat spread apart, and as a result, the α1-α2 and α2-α3 regions draw slightly closer to each other. This is the repression state. Upon binding of Cu(I)-CueR to DNA, the two DNA-binding domains of CueR get closer to each other, separating the two α1 helices even further, while simultaneously bringing the α2-α3 helices closer to the α1 helix. This motion suggests a squeezing mechanism underlying the conformations of the DNA-binding domain. It is likely that the latter state allows both the α1-α2 region and the α2-α3 region to coordinate directly to the DNA, and to facilitate transcription. In addition, continuous exchange between the apo-CueR, Cu(I)-CueR and Cu(I)-CueR-DNA forms of the protein takes place; at high copper concentrations, the equilibrium shifts toward the Cu(I)-CueR-DNA (activation) form. Figure 7 presents our suggested model for the CueR activation mechanism.

This research focused on the different conformational states of CueR in solution, and our findings provide insights into the mechanism through which CueR and Cu(I) activate and repress transcription within the copper-regulation machinery. Subsequent studies might seek to explore the structural effects of binding to a non-specific DNA sequence and a non-specific metal ion, thereby providing a deeper understanding of the transcription processes regulated by bacterial metallosensor proteins.

STAR★METHODS

Detailed methods are provided in the online version of this paper and include the following:

- KEY RESOURCES TABLES
- CONTACT FOR REAGENT AND RESOURCE SHARING
- EXPERIMENTAL MODEL AND SUBJECT DETAILS
- METHOD DETAILS
  - CueR Cloning & Expression Protocol
  - CueR Labeling Protocol
  - Cu(I) Addition
  - DNA Preparation for EPR Measurements
  - EPR Measurements
  - Models of Alternative Conformations
- DATA AND SOFTWARE AVAILABILITY

SUPPLEMENTAL INFORMATION

Supplemental Information includes six figures and one table and can be found with this article online at http://dx.doi.org/10.1016/j.str.2017.05.004.

AUTHOR CONTRIBUTIONS

H.S., A.N., S.A., N.B.-T., and S.R. designed the research. H.S., A.N., S.A., L.G.A., and Y.M. performed the research. H.S., A.N., and S.R. analyzed the data. Y.Z. and T.J.G. helped with the experimental procedures and contributed facilities. H.S., A.N., N.B.-T., and S.R. wrote the paper.

REFERENCES

Aitha, M., Moritz, L., Sahu, I.D., Sanyurah, O., Roche, Z., McCarrick, R.M., Lorigan, G.A., Bennett, B., and Crowder, M.W. (2015). Conformational dynamics of metallo-b-lactamase CcrA during catalysis investigated by using DEER spectroscopy. J. Biol. Inorg. Chem. 20, 585–594.

Andoy, N.M., Sarkar, S.K., Wang, Q., Panda, D., Benitez, J.J., Kalininskiy, A., and Chen, P. (2009). Single-molecule study of metalloregulator CueR-DNA interactions using engineered holiday junctions. Biophys. J. 97, 844–852.

Bhatnagar, J., Sircar, R., Borbat, P.P., Freed, J.H., and Crane, B.R. (2012). Self-association of the histidine kinase CheA as studied by pulsed dipolar ESR spectroscopy. Biophys. J. 102, 2192–2201.

Brown, N.L., Stoyanov, J.V., Kidd, S.P., and Hobman, J.L. (2003). The MerR family of transcriptional regulators. FEMS Microbiol. Rev. 27, 145–163.

Butala, M., Klose, D., Hodnik, V., Rems, A., Podlesek, Z., Klare, J.P., Anderluh, G., Busby, S.J.W., Steinhoff, H.J., and Zgur-Bertok, D. (2011). Interconversion between bound and free conformations of LexA orchestrates the bacterial SOS response. Nucleic Acids Res. 39, 6546–6557.

Changela, A., Chen, K., Holschen, J., Outten, C.E., O'Halloran, T.V., and Mondragon, A. (2003). Molecular basis of metal-ion selectivity and zeptomolar sensitivity by CueR. Science 301, 1383–1387.

Chen, K., Yuldasheva, J.E., Penner-Hahn, J.E., and O'Halloran, T.V. (2003). An atypical linear Cu(I)—S2 center constitutes the high-affinity metal-sensing site in the CueR metalloregulatory protein. J. Am. Chem. Soc. 125, 12088–12089.

Chen, T.Y., Santiago, A.G., Jung, W., Krzeminski, L., Yang, F., Martell, D.J., Helmann, J.D., and Chen, P. (2015). Concentration- and chromosome-organization-dependent regulator unbinding from DNA for transcription regulation in living cells. Nat. Commun. 6, 7445.

Edgar, R.C. (2004). MUSCLE: multiple sequence alignment with high accuracy and high throughput. Nucleic Acids Res. 32, 1792–1795.

Finney, L.A., and O'Halloran, T.V. (2003). Transition metal speciation in the cell: insights from the chemistry of metal ion receptors. Science 300, 931–936.

Freed, D.M., Lukasik, S.M., Sikora, A., Mokad, A., and Cafiso, D.S. (2013). Monomeric TonB and the Ton Box are required for the formation of a high affinity transporter-TonB complex. Biochemistry *52*, 2638–2648.

Giedroc, D.P., and Arunkumar, A.I. (2007). Metal sensor proteins: nature's metalloregulated allosteric switches. Dalton Trans. 3107–3120.

Grass, G., and Rensing, C. (2001). CueO is a multi-copper oxidase that confers copper tolerance in *Escherichia coli*. Biochem. Biophys. Res. Commun. *286*, 902–908.

Hubbell, W.L., Gross, A., Langen, R., and Lietzow, M.A. (1998). Recent advances in site-directed spin labeling of proteins. Curr. Opin. Struct. Biol. *8*, 649–656.

Hubbell, W.L., Lopez, C.J., Altenbach, C., and Yang, Z. (2013). Technological advances in site-directed spin labeling of proteins. Curr. Opin. Chem. Biol. *23*, 725–733.

Jeschke, G. (2012). DEER distance measurements on proteins. Annu. Rev. Phys. Chem. *63*, 419–446.

Jeschke, G. (2013). Conformational dynamics and distribution of nitroxide spin labels. Prog. Nucl. Magn. Reson. Spectrosc. *72*, 42–60.

Joseph, B., Morkhov, V.M., Yulikov, M., Jeschke, G., and Bordignon, E. (2014). Conformational cycle of the vitamin B_{12}ABC importer in liposomes detected by double electron-electron resonance (DEER). J. Biol. Chem. *289*, 3176–3185.

Joshi, C.P., Panda, D., Martell, D.J., Andoy, N.M., Chen, T.Y., Gaballa, A., Helmann, J.D., and Chen, P. (2012). Direct substitution and assisted dissociation pathways for turning off transcription by a MerR-family metalloregulator. Proc. Natl. Acad. Sci. USA *109*, 15121–15126.

Klare, J.P. (2013). Site-directed spin labeling EPR spectroscopy in protein research. Biol. Chem. *394*, 1281–1300.

Kumaraswami, M., Newberry, K.J., and Brennan, R.G. (2010). Conformational plasticity of the coiled coil domain of BmrR is required for bmr operator binding – the structure of unliganded BmrR. J. Mol. Biol. *398*, 264–275.

Ma, Z., Jacobsen, F.E., and Giedroc, D.P. (2009). Coordination chemistry of bacterial metal transport and sensing. Chem. Rev. *109*, 4644–4681.

Martell, D.J., Joshi, C.P., Gaballa, A., Santiago, A.G., Chen, T.Y., Jung, W., Helmann, J.D., and Chen, P. (2015). Metalloregulator CueR biases RNA polymerase's kinetic sampling of dead-end or open complex to repress or activate transcription. Proc. Natl. Acad. Sci. USA *112*, 13467–13472.

Narunsky, A., Nepomnyachiy, S., Ashkenazy, H., Kolodny, R., and Ben-Tal, N. (2015). ConTemplate suggests possible alternative conformations for a query protein of known structure. Structure *23*, 2162–2170.

Newberry, K.J., and Brennan, R.G. (2004). The structural mechanism for transcription activation by MerR family member multidrug transporter activation, N terminus. J. Biol. Chem. *279*, 20356–20362.

Outten, C.E., Outten, F.W., and O'Halloran, T.V. (1999). DNA distortion mechanism for transcriptional activation by ZntR, a Zn(II)-responsive MerR homologue in *Escherichia coli*. J. Biol. Chem. *274*, 37517–37524.

Outten, F.W., Outten, C.E., Hale, J.A., and O'Halloran, T.V. (2000). Transcriptional activation of an *Escherichia coli* copper efflux regulon by the chromosomal Mer homologue, CueR. J. Biol. Chem. *275*, 31024–31029.

Pettersen, E.F., Goddars, T.D., Huang, C.C., Couch, C.S., Greenblatt, D.M., Meng, E.C., and Ferrin, T.E. (2004). UCSF Chimera-a visualization system for exploratory research and analysis. J. Comput. Chem. *25*, 1605–1612.

Philips, S.J., Canalizo-Hernandez, M., Yildirim, I., Schatz, G.C., Mondragon, A., and O'Halloran, T.V. (2015). Allosteric transcriptional regulation via changes in the overall topology of the core promotor. Science *349*, 877–881.

Polyhach, Y., Bordignon, E., and Jeschke, G. (2011). Rotamer libraries of spin labelled cysteines for protein studies. Phys. Chem. Chem. Phys. *13*, 2356–2366.

Puljung, M.C., DeBerg, H.A., Zagotta, W.N., and Stoll, S. (2014). Double electron-electron resonance reveals cAMP-induced conformational change in HCN channels. Proc. Natl. Acad. Sci. USA *111*, 9816–9821.

Robinson, N.J., and Winge, D.R. (2010). Copper metallochaperones. Annu. Rev. Biochem. *79*, 537–562.

Sahu, I.D., McCarrick, R.M., Troxel, K.R., Zhang, R., Smith, H.J., Dunagan, M.M., Swartz, M.S., Rajan, P.V., Kroncke, B.M., Sanders, C.R., et al. (2013). DEER EPR measurements for membrane protein structures via bifunctional spin labels for lipodisp nanoparticles. Biochemistry *52*, 6627–6632.

Sali, A., and Blundell, T.L. (1993). Comparative protein modelling by satisfaction of spatial restraints. J. Mol. Biol. *234*, 779–815.

Stone, K.M., Townsend, J.E., Sarver, J., Sapienza, P.J., Saxena, S., and Jen-Jacobson, L. (2008). Electron spin resonance shows common structural features for different classes of EcoRI-DNA complexes. Angew. Chem. Int. Ed. *47*, 10192–10194.

Stoyanov, J.V., and Brown, N.L. (2003). The *Escherichia coli* copper-responsive copA promoter is activated by gold. J. Biol. Chem. *278*, 1407–1410.

Stoyanov, J.V., Hobman, J.L., and Brown, N.L. (2001). CueR (YbbI) of *Escherichia coli* is a MerR family regulator controlling expression of the copper exporter CopA. Mol. Microbiol. *39*, 502–512.

Wladron, K.J., Rutherford, J.C., Ford, D., and Robinson, N.J. (2009). Metalloproteins and metal sensing. Nature *460*, 823–830.

STAR★METHODS

KEY RESOURCES TABLES

REAGENT or RESOURCE	SOURCE	IDENTIFIER
Bacterial and Virus Strains		
BL21(DE3) Competent Cells	Novagen	69450
Chemicals, Peptides, and Recombinant Proteins		
isopropyl-β-D-thiogalactopyranoside	Calbiochem	420322; CAS: 367-93-1
Imidazole	ACROS Organics	3967450000; CAS:288-32-4
S-(2,2,5,5-tetramethyl-2,5-dihydro-1H-pyrrol-3-methyl) methanethiosulfonothiate (MTSSL)	TRC	O875000; CAS: 81213-52-7
DTT	Fisher BioReagents	BP172-25; CAS: 3483-12-3
Tetrakis(acetonitrile)copper(I) hexafluorophosphate	Sigma-Aldrich	346276; CAS: 64443-05-6
Critical Commercial Assays		
Pierce™ BCA Protein Assay Kit	Thermo Scientific	23227; Lot: QL224846
Oligonucleotides		
Primers for isolating CueR from *E.coli*: genomic DNA 5'-GCAGCGGCCTGGTGCCGCGCGGCAGCATGAA CATCAGCGATGTAGCAAAAATTACCGGCC-3' 3'-GTCCACCAGTCATGCTAGCCATATGTCACCCTG CCCGATGATGACAGCAGC-5'	Pubmed 11136469	AF318185
Primers for DNA for EPR measurements: 5'-CACCCGCAACTTAACTACAG-3' 3'-TTTAACGCAGTGACCGCAGG-5'	Pubmed 11136469	N/A
Recombinant DNA		
pET-28a(+) expression vector	Novagen	69864
Software and Algorithms		
DeerAnalysis 2013	Jeschke, 2012	http://www.epr.ethz.ch/software.html
2013 MMM	Polyhach et al., 2011 Jeschke, 2013	http://www.epr.ethz.ch/software.html
MODELLER version 9v8	Sali and Blundell, 1993	https://salilab.org/modeller/download_installation.html
UCSF Chimera version 1.10.1	Pettersen et al., 2004	https://www.cgl.ucsf.edu/chimera/download.html
ConTemplate version 1.0	Narunsky et al., 2015	http://bental.tau.ac.il/contemplate
MUSCLE version 8.47 T-COFFEE package	Edgar, 2004	http://www.drive5.com/muscle/downloads.htm
Other		
Protino® Ni-NTA agarose beads	Macherey-Nagel	1505/001; CAS:64-17-5
Microsep Advance Centrifugal Devices MWCO of 3K	Pall	MCP003C41
1.1/ 1.6 mm ID/OD capillary quartz tubes	Wilmad-LabGlass	WG-221T-RB

CONTACT FOR REAGENT AND RESOURCE SHARING

Further information and requests for resources and reagents should be directed to and will be fulfilled by the Lead Contact, Sharon Ruthstein (Sharon.ruthstein@biu.ac.il).

EXPERIMENTAL MODEL AND SUBJECT DETAILS

The CueR protein was expressed and purified from BL21 competent *E. coli* cells. The cells were transformed with pET-28a(+) expression vector comprising CueR gene were used as a representative wild-type strain, and all mutant strains were constructed in this background. Strains were constructed by Kanamycin resistance incorporated in pET-28a(+). Standard cell growth conditions were 37 ^{0}C incubation in LB liquid media, CueR expression was induced by isopropyl-β-D-thiogalactopyranoside .

METHOD DETAILS

CueR Cloning & Expression Protocol

CueR was isolated by PCR using *E.coli* genomic DNA with primers specific to the CueR N-terminal (5'-GCAGCGG CCTGGTGCCGCGCGGCAGCATGAACATCAGCGATGTAGCAAAAATTACCGGCC-3') and C-terminal (3'-GTCCACCAGTCATGC TAGCCATATGTCACCCTGCCCGATGATGACAGCAGC-5'). These primers also contain flanking sequences of the pET-28a(+) (Novagen) expression vector. The amplicon was cloned to the pET-28a(+) expression vector by the free ligation PCR technique. The same procedure was used to generate the different mutations, using specific primers containing the desired mutation. The CueR constructs were expressed in BL21(DE3) cells, which were grown to an optical density of 0.6-0.8 at 600 nm and induced with 1 mM isopropyl-β-D-thiogalactopyranoside (Calbiochem) for 3 hr at 37 ^{0}C. The cells were then harvested by centrifugation at 10,000 x g for 30 min, and pellets were subjected to three freeze-thaw cycles. Pellets were resuspended in NPI-10 buffer (50 mM NaH$_2$PO$_4$, 300 mM NaCl, 10 mM imidazole (ACROS Organics; pH 8.0) and sonicated by 5 bursts of 1 min each with a 1 min cooling period between each burst (40% amplitude). After sonication, the cells were centrifuged and the pellets were resuspended in NPI-10 buffer. The protein was then purified from the pellet suspension by Ni-NTA agarose beads (Macherey-Nagel), according to the manufacturer's protocol using the NPI-10 buffer as the elution buffer.

CueR purity was confirmed by 19% tricine SDS-PAGE using silver stain (see Supplemental Information, Figure S1B). Mass spectroscopy confirmed 95% purity.

CueR Labeling Protocol

The protein was labeled with S-(2,2,5,5-tetramethyl-2,5-dihydro-1H-pyrrol-3-methyl) methanethiosulfonothiate (MTSSL, TRC) at the targeted cysteines. CueR was initially incubated with 10 mM DTT (Fisher BioReagents) and Cu(I) ([CueR-monomer]:[Cu(I)]=1:20) overnight. DTT was removed by Microsep Advance Centrifugal Devices (Pall, ref. MCP003C41) up to 5 mL with a molecular weight cut-off (MWCO) of 3K in an NPI-10 lysis buffer three times at 3220 x g, 8 ^{o}C for 20 min. Cu(I) was added for a second time ([CueR-monomer]: [Cu(I)]=1:20) for 1 hr. The Cu(I) binding protects the metal-binding cysteines of CueR from spin labeling. MTSSL (MW=264.3 gr/mol) was added to the Cu(I)-CueR solution in a 1:50 = [Cu(I)-CueR]:[spin label] ratio, 50-fold molar excess of MTSSL, and then mixed overnight at 4 $^\circ$C in the dark. The free spin label was removed through the Microsep Advance Centrifugal Devices (Pall) up to 5 mL with MWCO of 3K in an NPI-10 buffer eight times at 3220 × g, 8 $^\circ$C for 20 min. This procedure ensures that no free spin label was left, and that the only selected cysteine residues are labeled. Moreover, during the centrifugation steps all Cu(I) was removed from the protein. CueR protein was concentrated and quantified by BCA assay (Pierce^{TM}). The final concentration of CueR protein after spin labeling was 10-15 μM.

Cu(I) Addition

After spin-labeling and all the centrifugation steps carried out for removal of free spin-labels from the solution, no Cu(I) ions were found in the protein solution. This was verified by adding 0.1 mM KCN to the solution and acquiring the CW-EPR spectra. The spectra in the presence and absence of KCN were similar. Moreover, run off transcription assays (Supplemental Information and Figure S1C) of the apo-protein solution did not show activity.

For EPR measurements: Cu(I) (Tetrakis (acetonitrile) copper(I) hexafluorophosphate) was added to the protein solution under nitrogen gas to preserve anaerobic conditions. Cu(I) was added up to 4-fold excess in relation to CueR monomer. This amount of Cu(I) was sufficient to enable us to observe major structural changes in the presence of DNA. No Cu(II) EPR signal was observed at any time.

DNA Preparation for EPR Measurements

A DNA PCR product containing 237 base pairs was used for the EPR measurements. This DNA fragment was isolated from the copA promoter and it includes a specific region known to bind CueR: -35/TTG ACCTTCCCCTTGCTGGAAGGTTTA/-10. PCR was done on *E. coli* genomic DNA using specific primers: primer(+) (5'-CACCCGCAACTTAACTACAG-3') and primer(-) (3'-TTTAACGCAGT GACCGCA GG-5').

EPR Measurements

The constant time four-pulse DEER experiment $\pi/2(\nu_{obs})$-τ_1-$\pi(\nu_{obs})$-T-$\pi(\nu_{pump})$-$(\tau_1+\tau_2$-T)-$\pi(\nu_{obs})$-$\tau_2(\nu_{obs})$-τ_2-echo was carried out at (80 ± 1.0K) on Q-band Elexsys E580 (equipped with a 2 mm probehead, and a bandwidth of 220 MHz). A two-step phase cycle was employed for the first pulse. The echo was measured as a function of T, while τ_2 was kept constant to eliminate relaxation effects. The observer pulse was set 60 MHz higher than the pump pulse. The observer $\pi/2$ and π pulses had a length of 40 ns (at zero dB attenuation), and the π pump pulse had a length of 40 ns as well; the dwell time was 20 ns. The observer frequency was 33.79 GHz. The samples were measured in 1.1/1.6 mm ID/OD capillary quartz tubes (Wilmad-LabGlass). Each DEER signal was acquired for 48-72 hr. The data were analyzed using the DeerAnalysis 2013 program, using Tikhonov regularization according to the L-curve criterion. The regularization parameter in the L-curve was optimized by examining the fit of the time domain data. The data presented are in principle after 3D homogeneous background subtraction. However, owing to the low protein concentration (about 10 μM), the homogeneous background contribution was negligible in most cases, and therefore the DEER data presented here are similar to the raw data.

MMM simulations were performed with a 2013 MMM program. MMM is a computational approach (Polyhach et al., 2011) used for deriving a rotamer library based on a coarse-grained representation of the conformational space of the spin label (Jeschke, 2013). This method describes spin labels by using a set of alternative conformations, which can be attached without serious clashes with atoms of other residues or cofactors. The rotamer library is derived from molecular dynamic simulation with a total length of 100 ns and at a temperature of 175 K, which is an estimate of the glass transition of a protein sample.

The structure of 1q05 misses 12 residues in two regions: the end of the C-terminus, and a loop connecting two helices at the end of each monomer (helices 4 and 5 in one monomer and helices 5 and 6 in the other monomer). The MMM program can only calculate the elastic network model of a complete structure. Thus, we used the MODELLER loop prediction tool installed on UCSF Chimera (Pettersen et al., 2004) to predict the locations of the missing residues, and used this structure in the elastic network model calculations.

Models of Alternative Conformations

The search for templates of alternative conformations of CueR was carried out using ConTemplate (Narunsky et al., 2015), which suggests alternative conformations for a query protein based on proteins that share the same conformation of the query and have multiple conformations in the PDB. ConTemplate also produces sequence alignment derived from the structural alignment between the query and structurally similar protein. We used this alignment, unless its quality was insufficiently high (e.g., large number of gaps), in which case we aligned the query and the template using MUSCLE (Edgar, 2004). Models of the alternative conformations were built using the templates, their alignment to the query and the MODELLER (Sali and Blundell, 1993) homology modeling tool.

Residues from the N-terminal binding domain were missing from the structures in PDB entries 1q08 and 1q0a, known structures of the ZntR. The spin label was attached to residues in this region and we modeled the missing residues to be able to compare the MMM simulations and the DEER measurements. Thus, the models obtained by these templates were built based on two templates; for the N-terminal we used 1q06, a CueR structure, and for the rest of the model we used the selected template. We modeled each chain separately and structurally aligned it to the relevant chain in the template in order to maintain the dimer configuration.

DATA AND SOFTWARE AVAILABILITY

DEER data were analyzed using the DeerAnalysis 2013 program, MMM simulations were performed with a 2013 MMM program and the search for templates of alternative conformations of CueR was carried out using ConTemplate. All software used are reported in Method Details and indicated in the Key Resources Table. The accession number for the CueR gene is AF318185 reported in PubMed 11136469. The DNA sequence (primer) was reported in PubMed 11136469 as well.